

# Quantum sensing of rotation velocity based on transverse field Ising model

Y. H. Ma<sup>1,2</sup> C. P. Sun<sup>1,2\*</sup>

<sup>1</sup>*Beijing Computational Science Research Center, Beijing 100193, China*

<sup>2</sup>*Graduate School of Chinese Academy of Engineering Physics, Beijing 100084, China*

We study a transverse-field Ising model (TFIM) in a rotational reference frame. We find that the effective Hamiltonian of the TFIM of this system depends on the system's rotation velocity. Since the rotation contributes an additional transverse field, the dynamics of TFIM sensitively responses to the rotation velocity at the critical point of quantum phase transition. This observation means that the TFIM can be used for quantum sensing of rotation velocity that can sensitively detect rotation velocity of the total system at the critical point. It is found that the resolution of the quantum sensing scheme we proposed is characterized by the half-width of Loschmidt echo of the dynamics of TFIM when it couples to a quantum system S. And the resolution of this quantum sensing scheme is proportional to the coupling strength  $\delta$  between the quantum system S and the TFIM, and to the square root of the number of spins  $N$  belonging the TFIM.

## I. INTRODUCTION

Quantum sensing is a kind of sensing scheme, which utilizes the quantum effects to enhance the measurement accuracy. Quantum gyroscope [1] is a kind of quantum sensor which makes use of quantum sensing schemes for rotation velocity measurement. For example, atom interferometer gyroscope (AIG) makes use of the interference of matter waves, and was first achieved in experiment in 1991[2]. Another quantum gyroscope is nuclear magnetic resonance gyroscope (NMRG), which detects the rotation velocity by detecting the precession frequency of the nuclear magnetic moment in the non-inertial system[3]. Both AIG and NMRG are quantum gyroscopes with high accuracy in measurement, and are used in high precision inertial navigation and military strategic system.

For a future quantum sensing scheme with much higher accuracy, we need to explore the roles which could be positive or negative of new quantum effects. The key to the quantum sensing scheme is the measurement accuracy, or in our case, the resolution for rotation velocity, which is physically reflected by the response of its dynamics to the rotation velocity of the system. In this paper, we study the dynamics of transverse field Ising model (TFIM) and found the Loschmidt echo (LE) of TFIM is sensitive to the rotation velocity at the critical point of quantum phase transition (QPT). In 2006, H.T.Quan, et al [4] found that when a TFIM couples with a quantum system S, and is turned into critical point of QPT, the quantum decoherence phenomena of system S will be significantly enhanced, which is characterized by the rapid decay of LE of the dynamics of TFIM around the critical point. For TFIM in non-inertial reference frame, its quantum phase transition behavior depends on the rotation velocity  $\Omega$  of the total system sensitively as the  $\Omega$  behaves as an external transverse field.

The QPT of TFIM in rotational reference frame will be affected directly by the rotation velocity of the sys-

tem, therefore it is feasible to achieve the measurement of rotation velocity through recording the QPT of TFIM. With this consideration, we designed a quantum sensing scheme to carry out rotation velocity measurements by detecting the QPT of TFIM in non-inertial reference frame. This paper is arranged as follows. In Sec. II, we study the Hamiltonian of the TFIM in non-inertial system and thus examine the response of the TFIM's LE to the rotation velocity  $\Omega$  of the system. In Sec. III, we propose a quantum sensing scheme based on TFIM in rotational reference frame, and give its resolution for rotation velocity  $\Omega$ . Conclusion of our results are given in Sec. IV.

## II. TRANSVERSE FIELD ISING MODEL IN NON-INERTIAL REFERENCE FRAME

In this section we consider a coupled spin system with an external field in a rotational reference frame. The Hamiltonian of the transverse field Ising model (TFIM) in the stationary system reads

$$H_0 = -J \sum_i (\sigma_i^z \sigma_{i+1}^z + \lambda \sigma_i^x), \quad (1)$$

where  $J$  and  $\lambda$  characterize the strengths of the inter-spin interaction and the coupling to the transverse field,  $\sigma_i^\alpha$  ( $\alpha \in \{x, y, z\}$ ) are Pauli operators defined in the state space of the  $i$ th particle. Note that, the critical point for quantum phase transition (QPT) of TFIM is  $\lambda_c = 1$  [4, 5], below which the TFIM will generate spontaneous magnetization. While a spin chain of TFIM is placed in a rotating system which rotates with an angle  $\theta(t)$  relative to the stationary reference frame, the time-dependent Hamiltonian of TFIM is

$$H(t) = -J \sum_i (\sigma_i^z(t) \sigma_{i+1}^z(t) + \lambda \sigma_i^x(t)), \quad (2)$$

where  $\sigma_i^\alpha(t)$  are Pauli matrices in the coordinate system which is relatively stationary with the TFIM. With the

\* cpsun@csrc.ac.cn

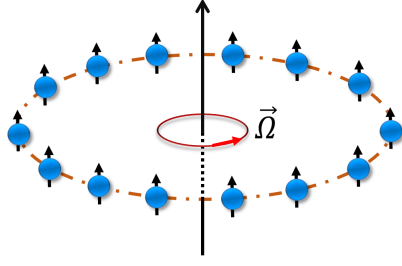


FIG. 1 (color online). Transverse field Ising model in rotation reference frame. The whole system is rotating around the axis with rotation velocity  $\vec{\Omega}$ .

help of rotation matrix  $D_{\vec{n}}(\theta)$ ,  $\sigma_i^\alpha(t)$  can be explicitly expressed by  $\sigma_i^\alpha$

$$\begin{pmatrix} \sigma_i^x(t) \\ \sigma_i^y(t) \\ \sigma_i^z(t) \end{pmatrix} = D_{\vec{n}}(\theta) \begin{pmatrix} \sigma_i^x \\ \sigma_i^y \\ \sigma_i^z \end{pmatrix}, \quad (3)$$

where  $\vec{n}$  is the direction vector of the rotation axis. When the system rotates counterclockwise in the x-direction, the rotation matrix is

$$D_x(\theta) = \begin{pmatrix} 1 & 0 & 0 \\ 0 & \cos \theta & -\sin \theta \\ 0 & \sin \theta & \cos \theta \end{pmatrix}. \quad (4)$$

In addition, we set  $\theta(0) = 0$ , so that  $H(0) = H_0$ .

The Schrodinger's equation in the rest reference frame for TFIM with rotation angle  $\theta(t)$  is  $i\hbar\partial\Psi/(\partial t) = H(\theta)\Psi$ , where  $\Psi$  is the wave function of TFIM in the rest reference frame. Obviously,  $\Psi' = R(\theta)\Psi$  represents the wave function of TFIM in the rotation reference frame, where  $R(\theta) = \exp(-i\vec{\theta} \cdot \vec{S}/2)$  is the rotation operator and  $\vec{S} = \sum_i \vec{s}_i$  is the total spin of the TFIM, while  $\vec{s}_i$  is the spin of the  $i$ th particle. Thus the Schrodinger's equation for  $\Psi'$  is

$$i\hbar\frac{\partial}{\partial t}\Psi' = \left( R(\theta) H(t) R^\dagger(\theta) - i\hbar R(\theta) \frac{\partial}{\partial t} R^\dagger(\theta) \right) \Psi'. \quad (5)$$

Eq. (5) indicates the effective Hamiltonian of the rotating TFIM in non-inertial reference is

$$H_{eff} = R(\theta) H(t) R^\dagger(\theta) - i\hbar R(\theta) \frac{\partial}{\partial t} R^\dagger(\theta). \quad (6)$$

For the system rotating around x axis,  $R(\theta)$  is

$$R_x(\theta) = \exp\left(-i\theta \sum_i \sigma_i^x/2\right). \quad (7)$$

It follows from Eqs. (2), (3), (4), (6) and (7) that the effective Hamiltonian for the rotating TFIM in non-inertial reference frame is obtained as

$$H_{eff} = -J \sum_i \left[ \sigma_i^z \sigma_{i+1}^z + \left( \lambda - \frac{\hbar\Omega}{2J} \right) \sigma_i^x \right]. \quad (8)$$

Here  $\Omega = d\theta/(dt)$  indicates the instantaneous rotation velocity of the total system. It is imagined from Eq. (1) that the rotation term in Eq. (8) can be regarded as an effective magnetic field interacting with spins in the x direction. For a single spin in TFIM, if we ignore the interaction with other spins, the effective Hamiltonian will be  $H_{eff}^i = -J \left( \lambda - \frac{\hbar\Omega}{2J} \right) \sigma_i^x$ , which is the same as that of the nuclear magnetic resonance(NMR). The physical meaning of this rotation term is similar to the Coriolis force, which is known as a basic non-inertial effect in classical mechanics.

In 2006, H.T.Quan et al. pointed out that [4], when TFIM couples with a two level quantum system S, the decoherence of S will be effectively enhanced while the TFIM is at its critical point for QPT. This phenomenon was proved to be directly related to the Loschmidt echo (LE) of the dynamical behavior of TFIM and has been observed experimentally[6, 7]. The Hamiltonian they used to describe the interaction between S and TFIM is

$$H(\lambda, \delta) = -J \sum_i \left( \sigma_i^z \sigma_{i+1}^z + \lambda \sigma_i^x + \delta |e\rangle \langle e| \sigma_i^x \right), \quad (9)$$

where  $J, \lambda, \sigma_i^\alpha$  ( $\alpha \in \{x, y, z\}$ ) are consistent with our previous explanation, and  $\delta$  is the coupling strength between TFIM and quantum system S. If the whole system is placed in a rotating system, there will be a correction to Hamiltonian in Eq. (9), which is

$$H(\tilde{\lambda}, \delta) = -J \sum_i \left( \sigma_i^z \sigma_{i+1}^z + \tilde{\lambda} \sigma_i^x + \delta |e\rangle \langle e| \sigma_i^x \right). \quad (10)$$

Here,

$$\tilde{\lambda} \equiv \lambda - \frac{\hbar\Omega}{2J}, \quad (11)$$

is defined as the total effective magnetic field which is modified by the rotation velocity  $\Omega$  of the non-inertial reference frame. To show the effect of the rotation on the dynamic of the system, we calculate the LE of TFIM [4] by taking  $N = 2000$ ,  $\delta = 0.01$ ,  $\lambda = 2$ ,  $\hbar = 1$ ,  $\Omega \in [0, 4J]$ . The result we get is demonstrated in FIG.2, which shows the relationship between LE and the effective magnetic field  $\tilde{\lambda}$ .

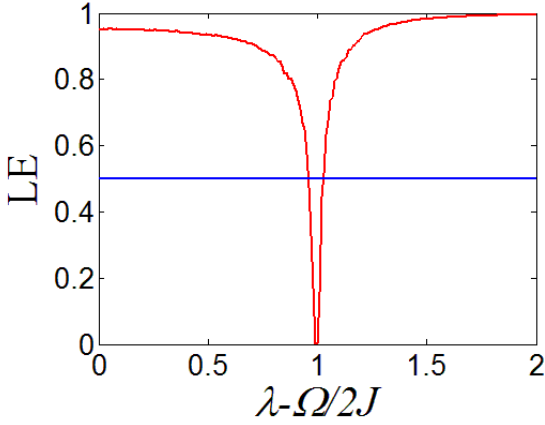


FIG. 2 (color online). Loschmidt echo as a function of rotation velocity  $\Omega$  for system with  $N = 2000$ ,  $\delta = 0.01$ .

This figure shows that around the critical point  $\tilde{\lambda} = 1$ , a tiny change of  $\Omega$  will cause rapid change of LE. The blue line in the figure marks  $L = 0.5$ , and the length of which inside the valley of LE represent the half-width of LE. The half-width of Loschmidt echo demonstrates the resolution of LE to the change of rotation velocity and will be further discussed in Section III.B

It is obvious in FIG.2 that a slight change of rotation velocity around the critical point for QPT of TFIM ( $\tilde{\lambda} = \lambda - \hbar\Omega/(2J) = 1$ ) results in a significant change in the value of LE, which indicates that the dynamics of TFIM is sensitive to the rotation velocity at the critical point of QPT. This suggests that TFIM can serve as a gyroscope in principle to measure the rotation velocity of a non-inertial system.

### III. QUANTUM SENSING SCHEME FOR ROTATION VELOCITY

Due to the sensitive dependence of the parameters  $(\lambda, \Omega)$  to QPT of TFIM, there comes an idea that the rotation of a system can be detected through the observation of TFIM's QPT. In another word, we propose a quantum sensing scheme which makes use of the quantum phase transition effect of TFIM. It can be seen in FIG. 2 that the significant response of LE to the change of rotation velocity occurs only near the critical point for QPT of TFIM.

To utilize the QPT effect to detect the rotation velocity sensitively, we need to keep  $\tilde{\lambda}$  near the critical point  $\lambda_c = 1$ . But for any rotation velocity to be measured,  $\tilde{\lambda}$  may be far away from  $\lambda_c$ , thus we need to adjust the magnetic field  $\lambda$  to ensure that  $\tilde{\lambda}$  fall in the range we are expecting. For the sensing scheme to be working properly, we need the magnetic field to be adjusted into the vicinity area of  $\tilde{\lambda}$ , but the problem is we do not know the value of  $\tilde{\lambda}$  in advance. To solve this problem, we present the following measurement scheme, which is illustrated in Fig. 3.

First, we use a pre-measuring gyroscope (PMG) to

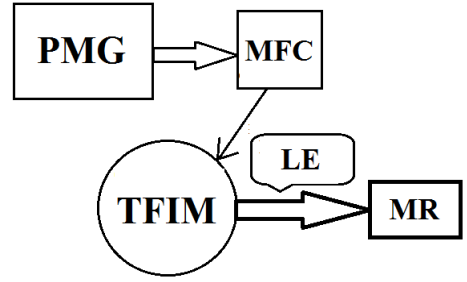


FIG. 3. Workflow of the quantum sensing scheme. The entire quantum sensing scheme needs to be achieved by the following modules. A pre-measuring gyroscope (PMR), which may be a MEMS gyroscope or a fiber optic gyroscope or other kinds of classical gyroscopes, a magnetic filed controller (MFC), a transverse field Ising model (TFIM) and circuitry to connect the entire system.

carry out a pre-measurement and send the result  $\Omega_0$  to the magnetic filed controller (MFC). Then the MFC will adjust the amplitude of the magnetic filed inside the module of TFIM to make the effective magnetic field  $\tilde{\lambda}$  in the vicinity of the critical point that  $\tilde{\lambda} \approx \lambda_c = 1$ . Let  $\sigma$  be the resolution of PMR, then the rotation velocity to be measured is in the following range

$$\Omega_1 \in [\Omega_0 - \sigma, \Omega_0 + \sigma]. \quad (12)$$

From Eqs. (11), (12), we obtain the magnetic field adjustment range of MFC

$$1 + \frac{\hbar}{2J} (\Omega_0 - \sigma) \leq \lambda \leq 1 + \frac{\hbar}{2J} (\Omega_0 + \sigma), \quad (13)$$

which is the key to make  $\tilde{\lambda}$  change in the vicinity of TFIM's critical point. When the QPT of TFIM occurs at  $\tilde{\lambda} = \lambda_c = 1$ , the LE will rapidly decay to zero. At the same time, the amplitude of the magnetic field is denoted as  $\lambda = \lambda_0$ . Thus the rotation velocity is measured as a result that

$$\Omega_1 = \frac{2J}{\hbar} (\lambda_0 - 1). \quad (14)$$

However, if we want to use this quantum sensing scheme to achieve a meaningful measurement for rotation velocity (the resolution is improved by TFIM compared with that of PMG, the distinguish-ability of TFIM's quantum phase transition to rotation velocity should be higher than that of PMR, which is to say

$$\Delta\Omega < \sigma, \quad (15)$$

where  $\Delta\Omega$  is the resolution of TFIM's QPT to rotation velocity.

For a quantum sensing scheme, its resolution is an important parameter, which indicates the minimum rotation velocity it can measure. In the above scheme we

have proposed, the resolution of TFIM's QPT to rotation velocity is characterized by the half-width of LE of the dynamics of TFIM. The smaller the LE's half-width is, the smaller rotation velocity the system can discern, and thus the higher resolution the system possesses. The exact expression for LE of the system with Hamiltonian in Eq. (9) was given in paper [4]. It can be seen from Eq. (10) that, while the entire system is placed in non-inertial reference frame, the Hamiltonian has the same form as in Eq. (9), except  $\lambda$  is replaced by  $\tilde{\lambda}$ . By using the constant variable method, we make the replacement  $\lambda \rightarrow \tilde{\lambda}$  for the solutions given in paper [4]. Thus the exact expression for  $L(\tilde{\lambda}, t)$  is naturally obtained as

$$L(\tilde{\lambda}, t) = \prod_{k>0} [1 - \sin^2(2\alpha_{\tilde{\lambda},k}) \sin^2(\varepsilon_e^{\tilde{\lambda},k} t)], \quad (16)$$

where

$$\alpha_{\tilde{\lambda},k} = \frac{1}{2} [\theta_{\tilde{\lambda},k}(0) - \theta_{\tilde{\lambda},k}(\delta)],$$

and

$$\theta_{\tilde{\lambda},k}(\delta) = \arctan \left\{ -\sin(ka) / [\cos(ka) - (\tilde{\lambda} + \delta)] \right\},$$

and the single quasiexcitation energy

$$\varepsilon_e^{\tilde{\lambda},k}(\delta) = 2J \sqrt{1 + (\tilde{\lambda} + \delta)^2 - 2(\tilde{\lambda} + \delta) \cos(ka)}.$$

Here, the Bloch wave vector  $k$  takes the discrete values  $2n\pi/(Na)$  ( $n = 1, 2, \dots, N/2$ ), where  $a$  and  $N$  are the lattice spacing and particle number of TFIM. We first make an analytical analysis by considering the partial sum with a cutoff wave vector  $K_c$ , thus

$$S(\tilde{\lambda}, t) = \ln L_c = - \sum_{k>0}^{K_c} |\ln F_k(\tilde{\lambda}, t)|, \quad (17)$$

where  $F_k(\tilde{\lambda}, t) = 1 - \sin^2(2\alpha_{\tilde{\lambda},k}) \sin^2(\varepsilon_e^{\tilde{\lambda},k} t)$ , and  $K_c$  can be expressed by a cutoff number  $N_c$  as  $K_c = N_c\pi/(Na)$ . When  $K_c a \ll 1$  ( $N_c \ll N$ )

$$S = - \frac{\delta^2 m \sin^2 \left[ 2J(1 - \tilde{\lambda})t/\hbar \right]}{(1 - \tilde{\lambda})^2 (1 - \tilde{\lambda} - \delta)^2}, \quad (18)$$

where

$$m \equiv \frac{4\pi^2 N_c (N_c + 1) (2N_c + 1)}{6N^2}. \quad (19)$$

It follows from Eqs. (17), (18) that

$$L_c = \exp \left\{ - \frac{\delta^2 m \sin^2 \left[ 2J(1 - \tilde{\lambda})t/\hbar \right]}{(1 - \tilde{\lambda})^2 (1 - \tilde{\lambda} - \delta)^2} \right\}. \quad (20)$$

Around the critical point for QPT, we set  $\epsilon = 1 - \tilde{\lambda} - \delta$ , as a result, if  $2J(\epsilon + \delta)t/\hbar \ll 1$  we have

$$L_c(\epsilon, t) = e^{-4\frac{\delta^2}{\epsilon^2} m J^2 t^2 / \hbar^2}. \quad (21)$$

To get the time-independent half-width of  $L_c$ , we define the characteristic time

$$t_0 \equiv \frac{\hbar}{2J}, \quad (22)$$

then we can calculate the half-width of  $L_c$ , which is defined as  $\epsilon_0$ , at  $t = t_0$

$$\frac{1}{2} = L_c(\epsilon_0, t_0) = e^{-\delta^2 m / \epsilon_0^2}. \quad (23)$$

In this case, the half-width of  $L_c$  is obtained as

$$\epsilon_0 = \delta \sqrt{m} / \sqrt{\ln 2} \approx \delta \sqrt{m}. \quad (24)$$

For the above analytical calculation, we further assume that the momentum cutoff  $K_c$  is an  $N$ -independent constant in the limit  $N \rightarrow \infty$ , i.e., we have

$$N_c = \alpha N, \quad (25)$$

where  $\alpha = K_c a / \pi$  is also an  $N$ -independent constant. Later we will verify this assumption and determine the value of  $\alpha$  via exact numerical calculation. Using relation (25), we find that the parameter  $m$  defined in Eq. (19) is expressed as

$$m = \frac{4\pi^2 \alpha N (\alpha N + 1) (2\alpha N + 1)}{6N^2} \approx \frac{4}{3} \pi^2 \alpha^3 N \equiv \eta N. \quad (26)$$

Thus, the Eq. (26) of the half-width  $\epsilon_0$  of  $L_c$  becomes

$$\epsilon_0 \approx \delta \sqrt{m} = \sqrt{\eta} \delta N^{\frac{1}{2}}. \quad (27)$$

Notice that  $\eta = 4\pi^2 \alpha^3 / 3$  is an  $N$ -independent parameter.

Equation. (27) implies that the half-width  $\epsilon_0$  or the behavior of  $L_c$  as a function of  $\tilde{\lambda}$  is determined by  $\delta N^{\frac{1}{2}}$ . This conclusion can be justified by numerical calculation

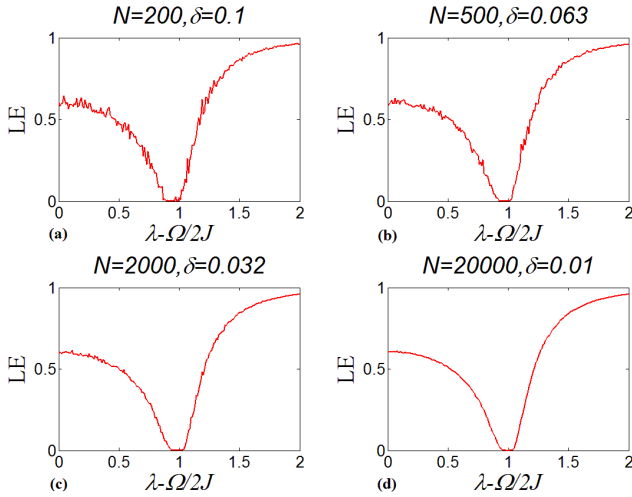


FIG. 4. (color online) Diagrams of Loschmidt echo as a function of rotation velocity  $\Omega$  in the case where  $\sqrt{N}\delta = \sqrt{2}$ . (a) System with  $N = 200$  and  $\delta = 0.1$ . (b) System with  $N = 500$  and  $\delta = 0.063$ . (c) System with  $N = 2000$  and  $\delta = 0.032$ . (d) System with  $N = 20000$  and  $\delta = 0.01$ . These curves of LE have the similar configuration.

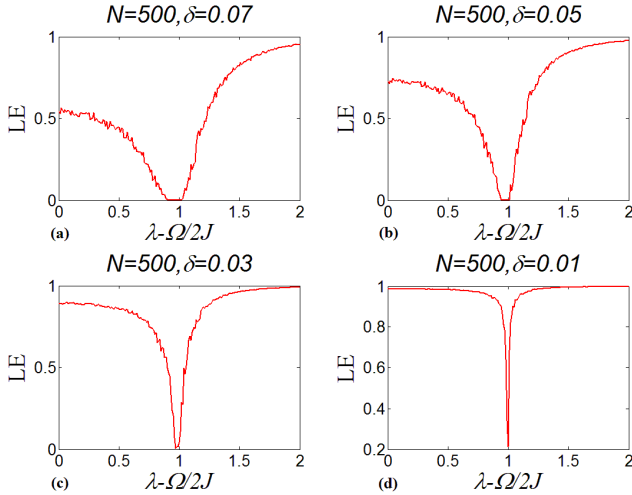


FIG. 5. (color online) Diagrams of Loschmidt echo as a function of rotation velocity  $\Omega$  for system with  $N = 500$ , and  $\delta$  respectively take 0.07, 0.05, 0.03, 0.01 in figure (a), (b), (c) and (d). These diagrams show that the valley of the curve become narrower when  $\delta$  is decreasing

by taking  $\lambda = 2$ ,  $\hbar = 1$ ,  $\Omega \in [0, 4J]$ , and the results are shown in Fig. 4, in which we illustrate  $L_c$  for the cases where the parameter  $\delta N^{\frac{1}{2}}$  is fixed at  $\sqrt{2}$  while  $N$  takes different values at 200, 500, 2000, and 20000. It is clearly shown that in these cases the behavior of  $L_c$  are quite similar. In Fig. 5 we show  $L_c$  for the cases with fixed value of  $N$  and different values of  $\delta$ . The calculation shows that the width of  $L_c$  decrease significantly with  $\delta$ . The numerical results in the two figures clearly confirm the results given by our analytical analysis, i.e., the behavior of  $L_c$  is determined by the parameter  $\delta N^{\frac{1}{2}}$  in the large- $N$  limit. Furthermore, with the help of Eq. (27) and the exact numerical solution of  $\epsilon_0$  given by Eq.

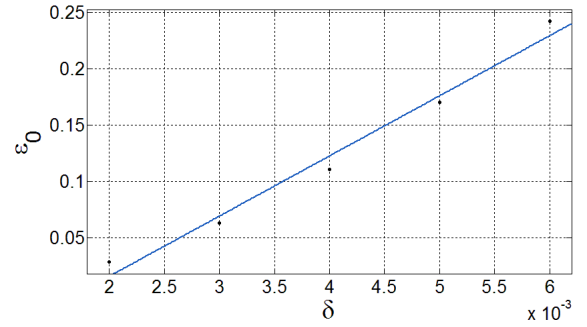


FIG. 6 (color online). Half-width of Loschmidt echo changes with different  $\delta$ . The black points in this figure is LE's half-width  $\epsilon_0$  given by numerical calculation, and the blue line is the fitting line of these points. It is obviously there exist a liner relationship between  $\epsilon_0$  and  $\delta$ , and the proportionality coefficient is given as  $\sqrt{\eta} = 0.375$ .

(16), we fit the value of parameter  $\alpha$  or  $\eta$  for system with  $N = 20000$ . As shown in Fig. 6, the fitting gives  $\sqrt{\eta} = 0.375$ . According to Eqs. (11), (27), the resolution of IGS is obtained as

$$\Delta\Omega = \frac{2J\epsilon_0}{\hbar} = 2\sqrt{\eta}\omega_0\delta\sqrt{N} = 0.75\omega_0\delta\sqrt{N}, \quad (28)$$

where  $\omega_0 \equiv J/\hbar$  is the characteristic coupling frequency of the spins' interaction. For  $\omega_0 \sim 1\text{Hz}$ ,  $\delta = 1 \times 10^{-5}$ ,  $N = 2000$ ,  $\Delta\Omega \approx 3.4 \times 10^{-4} (^{\circ})/s$ , accordingly, the constraint condition (15) becomes

$$\delta\sqrt{N} < 1.33 \frac{\sigma}{\omega_0}. \quad (29)$$

Here,  $\sigma$  is the resolution of the pre-measuring gyroscope.

#### IV. CONCLUSION

In summary, we have studied the rotation effect of the reference frame on the quantum phase transition (QPT) of the transverse field Ising model (TFIM). Since the rotation velocity will apply an equivalent magnetic field to the original transverse field, the dynamic evolution of the TFIM is sensitive to the rotation velocity of the reference frame at the critical point of TFIM; when we adjust the original transverse field to the vicinity of the critical point for QPT of TFIM, the Loschmidt echo will change significantly due to small changes of rotation velocity. This finding inspire us to design a quantum sensing scheme for measuring rotation velocity.

The quantum sensing scheme presented in this paper is composed of three steps. First, the approximate range of the rotation velocity is obtained by the pre-measurement. Then the magnetic field is adjusted based on the result of pre-measurement to tune the TFIM near the critical

point of QPT. Finally, the rotation velocity of the system is obtained by analyzing the feature of LE. Furthermore, we found the resolution of this quantum sensing scheme is proportional to  $\delta\sqrt{N}$ , where  $\delta$  is the coupling strength between quantum system S and TFIM, and  $N$  is the number of spins belongs to TFIM.

## ACKNOWLEDGMENTS

Y. H. Ma would like to thank Jin-fu Chen, Yi-nan Fang, Guo-hui Dong and Xin Wang in Beijing Computational Science Research Center for helpful discussion. This study is supported by the National Basic Research Program of China (Grant No. 2014CB921403 & No. 2016YFA0301201), the NSFC (Grant No. 11421063 & No. 11534002), and the NSAF (Grant No. U1530401).

- 
- [1] Armenise M N, Ciminelli C, Dell'Olio F, et al. Advances in gyroscope technologies[M]. Springer Science & Business Media, 2010.
  - [2] Barrett B, Geiger R, Dutta I, et al. The Sagnac effect: 20 years of development in matter-wave interferometry[J]. Comptes Rendus Physique, 2014, 15(10): 875-883.
  - [3] Walker T G, Larsen M S. Chapter Eight-Spin-Exchange-Pumped NMR Gyros[J]. Advances In Atomic, Molecular, and Optical Physics, 2016, 65: 373-401.
  - [4] Quan H T, Song Z, Liu X F, et al. Decay of loschmidt echo enhanced by quantum criticality[J]. Physical review letters, 2006, 96(14): 140604.
  - [5] Sachdev S. Quantum phase transitions[M]. John Wiley & Sons, Ltd, 2007.
  - [6] Zhang J, Peng X, Rajendran N, et al. Detection of quantum critical points by a probe qubit[J]. Physical review letters, 2008, 100(10): 100501.
  - [7] Zhang J, Cucchietti F M, Chandrashekar C M, et al. Direct observation of quantum criticality in Ising spin chains[J]. Physical Review A, 2009, 79(1): 012305.